REVISED

Cutoff Frequencies of Eccentric Waveguides*

by

H. Y. Yee and N. F. Audeh, member, IEEE

SUMMARY

28507

This paper discusses the uniform cylindrical waveguide formed by placing one conductor inside a conducting tube. Because of the complexity of the guide's cross section, the numerical technique of the point-matching method is adopted to solve the boundary-value problem. The formulations are carried out for the case when each of the conductors has an arbitrary cross section and also for the case when one of the conductors has a circular cross section.

The coaxial waveguide modes, in which the field components have angular variations, split into odd and even modes when the center conductor begins to shift axis to form the uniform eccentric waveguide. However, only even modes in the eccentric guide correspond to the coaxial modes with no angular variations. The dependence of the cutoff frequency on the eccentricity of the guide is determined numerically for even and odd TE and TM modes. Experimental results verify the theoretical calculations for TE modes.

Author

*This research work was supported by the National Aeronautics and Space Administration and was partially funded under NsG-381; also, by the Army Missile Command under Contract DA-01-021-AMC-14441(Z).

Mr. Yee is with the Department of Electrophysics of Polytechnic Institute of Brooklyn, New York, on a leave of absence from the University of Alabama Research Institute, Huntsville, Alabama.

Mr. Audeh is with the University of Alabama Research Institute, Huntsville, Alabama.

1. INTRODUCTION

A two-conductor waveguide in which one conductor encloses the other and each has an arbitrary cross section presents an interesting problem for the application of the point-matching technique. A special case of this guide is when each of the two conductors has a circular cross section; such a circular eccentric guide has been used as an adjustable quarter-wave transformer for TEM wave modes of propagation.[1] The characteristic impedance of this transmission line decreases as the eccentricity between the inner and the outer conductors increases. When operating at relatively high frequencies, however, it should be taken into account that high order modes may be excited.

Recently, the point-matching technique has been utilized to solve eigenvalue problems in many areas of engineering science.[2-5] The boundary conditions of a two-dimensional problem are imposed at a finite number of points around the periphery. Under this assumption, the partial differential equation of the problem can be reduced to a system of algebraic equations. This method is convenient especially when a high speed digital computer is available. In this paper, the cutoff frequencies of circular eccentric waveguides will be calculated by the point-matching method for the lowest and the next higher order TE and TM wave modes, and the results are plotted for several geometrical configurations.

It is observed that each of the degenerate wave modes (with angular-varying field distribution) in the circular coaxial waveguides are split into two modes when the guide becomes eccentric, namely: the even and the odd modes. The even mode is assigned to the mode for which the longitudinal field component is symmetric with respect to the line of eccentricity,[†] while the odd mode is assigned to the mode for which the longitudinal component is anti-symmetric with respect to the line of eccentricity. Each of the modes with no angular-varying field in the coaxial waveguides has only even modes in eccentric waveguides.

[†] The line of eccentricity is defined as the line joining the centers of the two conductors.

Cutoff frequencies of both the lowest order even and odd TM wave modes are decreasing with increasing eccentricity. The cutoff frequency of the lowest order even TE mode is increasing with increasing eccentricity. There is, however, very little change in cutoff frequency of the lowest order odd TE mode if the ratio of the radii of the outer and inner conductors is equal to three or larger.

The objective of this paper is twofold: 1) to obtain data of several circular eccentric waveguides of different geometrical configurations, 2) to show that the eigenvalue problem of this type of two-conductor waveguide, in which each conductor is arbitrary in cross-sectional shape, can be solved by the point-matching method.

The measured data for two circular eccentric guides verify the theoretical values.

2. THEORETICAL FORMULATION

Consider a two-conductor waveguide in which one conductor encloses the other. Let the guide be oriented such that the z-axis is enclosed by the inner conductor, and the cross section of the guide be symmetrical with respect to the x-axis as shown in Fig. 1(a). Let a time-harmonic [exp (jωt)] electromagnetic wave propagate between the two conductors in the positive z-direction. The solutions of the scalar Helmholtz equation, for the even and odd modes may be written in terms of coaxial wave modes as follows:[6]

$$\psi_e = \sum_{n=o}^{\infty} [A_{en} J_n(kr) + B_{en} Y_n(kr)] \cos n\theta \tag{1}$$

$$\psi_o = \sum_{n=1}^{\infty} [A_{on} J_n(kr) + B_{on} Y_n(kr)] \sin n\theta \tag{2}$$

where the subscripts e and o stand for even and odd respectively, n is an integer, and r and θ are the polar coordinates. J_n and Y_n are the nth order Bessel functions of the first and second kinds respectively. The quantities A_n and B_n are constants to be determined by the boundary conditions. The cutoff wave number k, is given by

$$k^2 = \omega^2 \mu_o \epsilon_o - k_z^2$$

where μ_o and ϵ_o are the constitutive parameters of free space, ω is the operating angular frequency, and $k_z = 2\pi/\lambda_g$, is the propagation constant. The wave function $\psi = H_z$ for TE wave modes, and $\psi = E_z$ for TM wave modes. The wave function ψ must satisfy either Dirichlet or Neumann boundary conditions. With the known longitudinal field components H_z or E_z the transverse field components can be computed by:

$$\overline{E}_t = (jk_z/k^2)\,[-\nabla_t E_z + (\omega\mu_o/k_z)\,\overline{z} \times (\nabla_t H_z)] \tag{3}$$

$$\overline{H}_t = (-jk_z/k^2)\,[(\omega\epsilon_o/k_z)\,\overline{z} \times (\nabla_t E_z) + \nabla_t H_z] \tag{4}$$

where $\overline{z}$ is the unit vector in the z-direction, and ∇_t is the transverse gradient operator. The cutoff wave number k and the expansion coefficients A_n and B_n for each wave mode are found by requiring that the wave function ψ satisfies the boundary conditions. Thus, by means of (1) - (4) the field inside the waveguide is completely described, and the power transfer, the attenuation constant due to the finite conductivity of the walls, and other information about the guide can be determined by numerical techniques.

Assuming that the series in (1) and (2) converge rapidly and uniformly for the cases under consideration, the wave functions may be approximated by a finite number of terms, i.e.

$$\psi_e = \sum_{n=o}^{N-1} [A_{en} J_n(kr) + B_{en} Y_n(kr)] \cos n\theta \tag{5}$$

$$\psi_o = \sum_{n=1}^{N} [A_{on} J_n(kr) + B_{on} Y_n(kr)] \sin n\theta \tag{6}$$

The point-matching technique requires (5) or (6) to satisfy the boundary conditions at a finite number of points, namely, 2N points. Let the points (r_1, θ_1), (r_2, θ_2), ... (r_N, θ_N) be a set of chosen points around the outer cross-sectional contour, and (r_{N+1}, θ_{N+1}), (r_{N+2}, θ_{N+2}), ... (r_{2N}, θ_{2N}) be the corresponding set of chosen points around the inner cross-sectional contour. The boundary conditions at these points for TM modes require

$$\sum_n [A_n J_n(kr_m) + B_n Y_n(kr_m)] \begin{matrix}\cos\\ \sin\end{matrix} n\theta_m = 0 \tag{7}$$

and for TE modes require

$$\bar{n} \cdot \nabla_t \sum_n [A_n J_n(kr_m) + B_n Y_n(kr_m)] \begin{matrix}\cos\\ \sin\end{matrix} n\theta_m = 0 \tag{8}$$

where $m = 1, 2, 3, \ldots 2N$, and $\bar{n}$ is the unit vector normal to the surface. The limits of the summations are the same as those of (5) and (6). The constants A_n and B_n with neither one of the subscripts (e, o) implies either even or odd. Also, the upper and lower functions in (7) and (8) will always designate the even and odd wave modes respectively. In a more precise form, (8) may be written as

$$\begin{aligned}&\sum_n \{kr_m [A_n J'_n(kr_m) + B_n Y'_n(kr_m)] \begin{matrix}\cos\\ \sin\end{matrix} n\theta_m \\ &\mp \tan\alpha_m [A_n J_n(kr_m) + B_n Y_n(kr_m)] \begin{matrix}\sin\\ \cos\end{matrix} n\theta_m \} = 0\end{aligned} \tag{8a}$$

where $\cos\alpha_m = \bar{n} \cdot \bar{r}_m$ for $m = 1, 2, \ldots, N$; $\cos\alpha_m = -\bar{n} \cdot \bar{r}_m$ for $m = N+1, N+2, \ldots, 2N$; and $\bar{r}_m$ is the unit vector in the r-direction at point (r_m, θ_m) as shown in Fig. 1(b). The above formulations ensure the wave functions satisfying the boundary conditions simultaneously at the chosen points on the outer and the inner cross-sectional contours. Each of (7) and (8a) forms a system of 2N homogeneous algebraic equations of 2N expansion coefficients A_n and B_n with the cutoff wave number k as the parameter. To obtain non-trivial solutions of A_n and B_n, the determinant of these coefficients must be zero. That is,

$$D(k) = \det |d_{ij}| = 0 \tag{9}$$

where

$$d_{ij} = J_i(kr_j) \begin{matrix}\cos\\ \sin\end{matrix}\ i\theta_j \tag{9a}$$

$$d_{ij} = Y_{i-N}(kr_j) \begin{matrix}\cos\\ \sin\end{matrix}\ (i-N)\,\theta_j \tag{9b}$$

for TM modes; and

$$d_{ij} = kr_j \begin{matrix}\cos\\ \sin\end{matrix}\ i\theta_j\, J_i'(kr_j) \mp i \tan\alpha_j \begin{matrix}\sin\\ \cos\end{matrix}\ i\theta_j\, J_i(kr_j) \tag{9c}$$

$$d_{ij} = kr_j \begin{matrix}\cos\\ \sin\end{matrix}\ (i-N)\,\theta_j\, Y_{i-N}'(kr_j) \mp (i-N) \tan\alpha_j \begin{matrix}\sin\\ \cos\end{matrix}\ (i-N)\,\theta_j\, Y_{i-N}(kr_j) \tag{9d}$$

for TE modes;

where for (9a) and (9c)

$$i = \begin{cases} 0, 1, 2, \ldots, N-1 \\ 1, 2, 3, \ldots, N \end{cases}$$

and for (9b) and (9d)

$$i = \begin{cases} N, N+1, \ldots, 2N-1 \\ N+1, N+2, \ldots, 2N \end{cases}$$

and $\qquad j = 1, 2, \ldots, 2N$

Equation (9) will be referred to as the point-matching characteristic equation. The roots of (9) are the values of k which are infinite in number, each of which corresponds to a wave mode. Having determined the cutoff wave number for a specific mode, the expansion coefficients A_n and B_n can readily be found from (7) and (8a).

It should be noted that the chosen points around the inner cross-sectional contour (inner points) depend on the outer points and vice versa. The dependence is that for a polar coordinate θ_m of an outer point, there is an inner point which has the same polar coordinate. That is, $\theta_m = \theta_{N+m}$ where $m = 1, 2, \ldots, N$. Under this condition, (9) yields exact solutions when applied to the circular coaxial guide.

3. ONE CONDUCTOR WITH CIRCULAR CROSS SECTION

If one of the cross-sectional contours is circular, not only is the previous analysis applicable, but also (9) can be reduced from a determinant of order 2N to a determinant of order N, with the same accuracy or better. Due to the limited capacity of a digital computer, the evaluation of the smaller determinant is easier and more economical.

Let the z-axis be collinear with the axis of the circular conducting tube of radius a. The boundary conditions can be satisfied exactly at the boundary of $r = a$ by setting $E_z = 0$ and $E_\theta = 0$ for TM and TE modes respectively. The boundary conditions on the other conductor with general cross section, where r depends on θ, are imposed point-wise.

Consider the TM modes first, the wave functions (5) and (6) are still valid for this waveguide. The boundary conditions at $r = a$ require that

$$B_n = -A_n J_n(ka)/Y_n(ka) \tag{10}$$

Substituting (10) into (5) and (6), and matching the boundary conditions at finite number of points only at the general cross-sectional contour yield

$$\sum_n \{[J_n(kr_m)\, Y_n(ka) - J_n(ka)\, Y_n(kr_m)] \left(\begin{matrix}\cos\\ \sin\end{matrix}\; n\theta_m\right)/Y_n(ka)\}\, A_n = 0 \tag{11}$$

where (r_1, θ_1), (r_2, θ_2), ..., (r_N, θ_N) are N points properly chosen around the general contour. The limits of the summation are between 0 and (N - 1) for the even modes and between 1 and N for the odd modes.

Since the factor $1/Y_n(ka)$ is the same for every column of the matrix inside the braces of (11), the determinant of this matrix being equal to zero is equivalent to setting

$$D(k) = \det |d_{mn}| = 0 \tag{12}$$

where $$d_{mn} = [J_n(kr_m)\, Y_n(ka) - J_n(ka)\, Y_n(kr_m)] \begin{matrix}\cos\\ \sin\end{matrix}\, n\theta_m$$

and $$1/Y_n(ka) = 0 \tag{13}$$

Observe that the order of the determinant of the point-matching characteristic equation is N. Evidently, it is easier to evaluate (12) than the equations in (9). The root of (13) is $k = 0$ which is the solution of the TEM mode

For the TE wave modes, the equation corresponding to (10) is given by

$$B_n = - A_n\, J'_n(ka)/Y'_n(ka) \tag{14}$$

Substituting (14) into (5) and (6) and again using the point-matching method on the general cross-sectional contour yields

$$\begin{aligned} &\sum_n \{[J'_n(kr_m)\, Y'_n(ka) - J'_n(ka)\, Y'_n(kr_m)]\, kr_m \left(\begin{matrix}\cos\\ \sin\end{matrix}\, n\theta_m\right)/Y'_n(ka) \\ &\mp \tan\alpha_m\, [J_n(kr_m)\, Y'_n(ka) - J'_n(ka)\, Y_n(kr_m)]\, n\left(\begin{matrix}\sin\\ \cos\end{matrix}\, n\theta_m\right)/Y'_n(ka)\}\, A_n = 0 \end{aligned} \tag{15}$$

where $m = 1, 2, 3, \ldots N$

The limits of the summation are the same as for TM modes. Equation (15) is similar in form to (11), and by the same reasoning, the matrix inside the braces of (15) leads to the form of (12) with

$$\begin{aligned} d_{mn} = &[J'_n(kr_m)\, Y'_n(ka) - J'_n(ka)\, Y'_n(kr_m)]\, kr_m \begin{matrix}\cos\\ \sin\end{matrix}\, n\theta_m \\ &\mp \tan\alpha_m\, [J_n(kr_m)\, Y'_n(ka) - J'_n(ka)\, Y_n(kr_m)]\; n \begin{matrix}\sin\\ \cos\end{matrix}\, n\theta_m \end{aligned}$$

and $$1/Y'_n(ka) = 0$$

Again $k = 0$ is the solution for the TEM mode.

With the cutoff wave number determined, the expansion coefficients A_n and B_n can be computed by (10), (11), (14), and (15). It is easy to see that (11) and (15) are reducable to exact solutions when applied to circular coaxial waveguides.

4. COMPARISON OF EXPERIMENTAL AND THEORETICAL RESULTS

To verify the correctness of the previous formulations, two circular eccentric waveguides were investigated experimentally. One of the eccentric waveguides [see Fig. 2] under consideration is made of two circular copper tubes with radii $a = 0.475$ cm and $b = 1$ cm, the distance between the two axes $L = 0.315$ cm. (Let this be designated as number 1 waveguide.) The dimensions of the other waveguide (number 2) are $a = 0.15875$ cm, $b = 1$ cm, and $L = 0.379$ cm. The cutoff frequencies are measured by the resonant-frequency method[7], by which the guide is shorted on both ends, thus, forming a resonant cavity. The waveguide cavities of these two examples are 15.48 cm in length. The energy was fed through a rectangular slit.

From the field distributions [see Fig. 3], if the slit is placed radially outward at the largest dimension of the guide as shown in Fig. 4(a), the energy fed into the guide induces the odd TE_{11} (denoted by OTE_{11}). If the slit is displaced by an angle of 90° from the position of the guide's largest dimension as in Fig. 4(b), the even TE_{11} (ETE_{11}) is induced. The normalized cutoff wave numbers ka, are tabulated in Tables I and II for the No. 1 and the No. 2 guides, respectively. The measured data show in most cases better than two-place accuracy. The error is partly due to the physical construction of the eccentric guides, otherwise, the accuracy is expected to be better. This can be seen when $L = 0$ (coaxial guide) in No. 1, for which the theoretical cutoff frequency is 6.5513 Gc while the experimental value is 6.5505 Gc.

The two waveguide cavities were also examined at frequencies from 4 Gc up to cutoff (6.546 Gc and 7.237 Gc for OTE_{11} modes for No. 1 and No. 2 guides respectively), and no resonance was observed.

The theoretical values in Table I and Table II are computed by (12) with the z-axis being collinear with the axis of the waveguide's inner circular tube. Eleven points were chosen on the outer cross-sectional contour and were approximately evenly distributed. The calculated values are believed to have three-place accuracy since, for example, the values of ka, 0.65263 and 0.65269 of the OTE_{11} mode for the No. 1 guide are calculated by eleven points and fifteen points respectively. More evidence will appear later concerning the accuracy of the computation.

Table I - Comparisons of cutoff wave numbers, ka, of No. 1 waveguide.

	OTE_{11}	ETE_{11}
Measured	0.6512	0.7205
Calculated	0.6526	0.7200

Table II - Comparisons of cutoff wave numbers, ka, of No. 2 waveguide.

	OTE_{11}	ETE_{11}
Measured	0.2779	0.2840
Calculated	0.2791	0.2849

5. CUTOFF FREQUENCIES OF ECCENTRIC WAVEGUIDES

As shown in the last sections, the experimental data of eccentric waveguides substantiate that the point-matching characteristic equation (12) is applicable for calculating the cutoff frequencies of TE wave modes. The validity of (12) for TM wave modes will be demonstrated in Section 6.

In Fig. 5 through Fig. 10, the normalized cutoff wave numbers ka of eccentric waveguides are plotted vs. the normalized eccentricity L/a with the radius ratio b/a considered as the parameter. For the TE modes, the radius ratios of 1.5, 2.0, 3.0 and 4.0 are shown, while for the TM modes the ratios of 2.0 and 4.0 only are shown. The eccentricity varies from the minimum value of zero to the maximum value.

The behavior of the cutoff frequencies with varying eccentricity is irregular for all higher order modes. However, the cutoff frequency decreases with increasing of eccentricity for both lowest order odd and even TM modes, i.e. the OTM_{11} and the ETM_{10}. This phenomenon is reversed for the ETE_{11} mode. The eccentricity however, has little effect on the cutoff characteristics of the OTE_{11} mode except when the two conductors are almost touching. In this case, the cutoff frequency becomes lower than that of the coaxial guide. The pairs OTE_{mn} and ETE_{mn}, and OTM_{pq} and ETM_{pq} of the eccentric guides are split from the degenerate TE_{mn} and TM_{pq} modes of the coaxial waveguide with the same radius ratio, respectively. However, the TE_{mo} and TM_{mo} modes of the coaxial guides correspond only to the even modes in the eccentric guides.

The plots in Fig. 5 through 10 are based on the calculated values of (12) with three-place accuracy or better. The cutoff wave numbers of OTE_{11} mode for b/a = 1.5 are computed by (12) using 11, 13, 15 and 18 points on the boundary and the results are shown in Table III. Those for ETE_{11} mode of the same guide computed by 11 and 18 points are shown in Table IV. The chosen points on the outer contour are approximately evenly distributed.

Table III - Comparison of cutoff wave numbers ka of OTE_{11} mode with $b/a = 1.5$, calculated by 11, 13, 15 and 18 points.

No. of Points \ L/a	0.1	0.2	0.3	0.4	0.45
11	0.80415	0.80102	0.79446	0.77616	-------
13	0.80415	0.80102	0.79450	0.78068	0.76631
15	0.80415	0.80102	0.79450	0.78067	0.76581
18	0.80415	0.80102	0.79450	0.78069	0.76634

Table IV - Comparison of cutoff wave number ka of ETE_{11} mode with $b/a = 1.5$, calculated by 11 and 18 points.

No. of Points \ L/a	0.1	0.2	0.3	0.4	0.5
11	0.81224	0.83544	0.88145	0.96824	1.1459
18	0.81224	0.83545	0.88147	0.96906	1.1459

For TM wave modes, the differences between the values calculated by 11 and 18 points are at most in the fifth place. It is observed that the convergence of the series solution is more rapid if the ratio of radii b/a and the eccentricity L/a are smaller.

6. DISCUSSION

The point-matching technique is a convenient method for computing the cutoff wave numbers of eccentric waveguides. The point-matching characteristic equation (12) was verified experimentally for TE wave modes. The validity of (12) for TM wave modes can be verified from the boundary conditions point of view.

Substituting the particular wave number of TM mode under consideration [calculated by (12)] into (11), the expansion coefficients A_n can then be determined algebraically. Rewriting (11) with r_c replacing r_m yields,

$$\sum_n [J_n(kr_c) Y_n(ka) - J_n(ka) Y_n(kr_c)]^{\cos}_{\sin} n\theta_m [A_n/Y_n(ka)] = 0 \tag{16}$$

where ka and A_n are known constants. r_c, function of θ, describes the curve where the boundary conditions [i.e. $\psi(r_c, \theta) = 0$] is satisfied beside at $r = a$ imposed previously [see (10)]. It can be seen that the function r_c given by (16), represents a single-valued closed contour. From (5), (6) and (10) through (12) obviously r_c passes the chosen points on the general cross-sectional contour. If the intervals between the chosen points are made sufficiently small, (smaller than the cutoff wavelength) the deviation between the actual cross-sectional contour and that described by (16) is expected to be small. The cutoff wave numbers of TM wave modes calculated by (12) will give as good an accuracy as desired.

From the previous analysis, it is seen that (12) is obtained by matching the boundary conditions exactly at the circular cross-sectional contour and approximately at the general cross-sectional contour. The limitation of using (12) on the general contour are the same as those discussed in Reference (5). Numerical computations show that (12) fails to determine the cutoff frequencies of TE modes for cross-sections with re-entrant corners.

To verify the formulation of Section 2, the cutoff wave numbers ka of ETE_{11} modes for circular eccentric waveguides are calculated by (9) and compared with those obtained by (12) as shown in Table V. The calculations are using the same set of chosen points as discussed in Section 2. Observe that (9) is valid but the accuracy is not as good as that obtained by using (12) especially when the eccentricity is large.

Table V - Comparison of ka of ETE_{11} calculated by (9) and (12).

L/a / Eq.	b/a = 1.5			b/a = 3	
	0.1	0.2	0.3	0.4	0.8
(9)	0.81222	0.83140	0.86601	0.51833	0.53204
(12)	0.81224	0.83544	0.88145	0.51827	0.53304

In the analysis in Sections 2 and 3 are formulas for the computation of waveguides with cross sections more complex than that of the eccentric guides. Cutoff frequencies computed in Sections 4 and 5 serve as an example of the applications of the point-matching technique. With the expansion coefficients found as outlined, the attenuation constant due to the finite conductivity of the conductors may be estimated.[8]

REFERENCES

1. Moreno, Theodore, "Microwave Transmission Design Data," Dover Publications, Inc., New York, (1958), pp. 106-107.

2. Conway, H. D., "The approximate analysis of certain boundary-value problems," J. Appl. Mech., vol. 27, (1960), pp. 275-277.

3. Leissa, A. W. and F. W. Niedenfuhr, "A study of the cantilevered square plate subjected to a uniform loading," J. Aerospace Sci., vol. 29, (1962), pp. 162-169.

4. Mullin, C. R., R. Sandburg, and C. O. Velline, "A numerical technique for the determination of scattering cross sections of infinite cylinders of arbitrary geometrical cross sections," IEEE Trans. on Antennas and Propagation, vol. AP-13, (January 1965), pp. 141-149.

5. Yee, H. Y. and N. F. Audeh, "Uniform waveguides with arbitrary cross sections considered by the point-matching method," IEEE Trans. on Microwave Theory and Techniques, vol. MTT-13, (November 1965), pp. 847-851.

6. Ramo, Simon and John R. Whinnery, "Fields and Waves in Modern Radio," John Wiley and Sons, Inc., New York, 2nd Ed., (1953), p. 364.

7. Audeh, N. F. and H. Y. Yee, "Measurement of cutoff frequencies," IEEE Trans. on Microwave Theory and Techniques, vol. MTT-13, (November 1965), p. 878-879.

8. Yee, H. Y. and N. F. Audeh,"Attenuation constants of waveguides with general cross sections," to appear in IEEE Trans. on Microwave Theory and Techniques, vol. MTT-14, (May 1966).

FIGURE CAPTIONS

Fig. 1 (a) The geometry of the two-conductor waveguide under consideration.

(b) The angle α at the chosen points.

Fig. 2 The cross section of the eccentric waveguide.

Fig. 3 (a) The field configuration of the ETE_{11} mode.

(b) The field configuration of the OTE_{11} mode.

Fig. 4 (a) The coupling hole for exciting OTE_{11} mode.

(b) The coupling hole for exciting ETE_{11} mode.

Fig. 5 Cutoff wave numbers of eccentric guide with $b/a = 1.5$ for TE modes.

Fig. 6 Cutoff wave numbers of eccentric guide with $b/a = 2.0$ for TE modes.

Fig. 7 Cutoff wave numbers of eccentric guide with $b/a = 3.0$ for TE modes.

Fig. 8 Cutoff wave numbers of eccentric guide with $b/a = 4$ for TE modes.

Fig. 9 Cutoff wave numbers of eccentric guide with $b/a = 2.0$ for TM modes.

Fig. 10 Cutoff wave numbers of eccentric guide with $b/a = 4$ for TM modes.

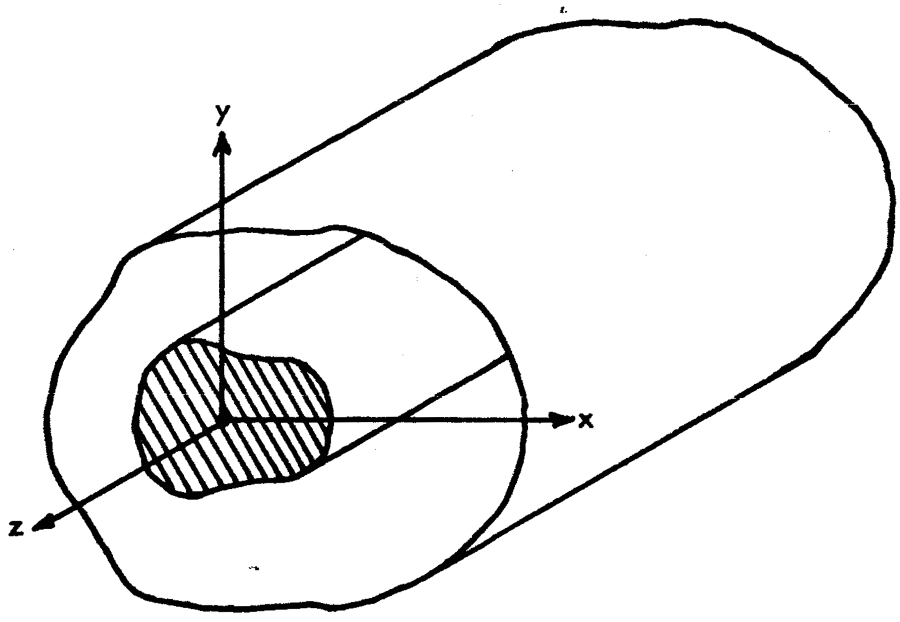

(a)

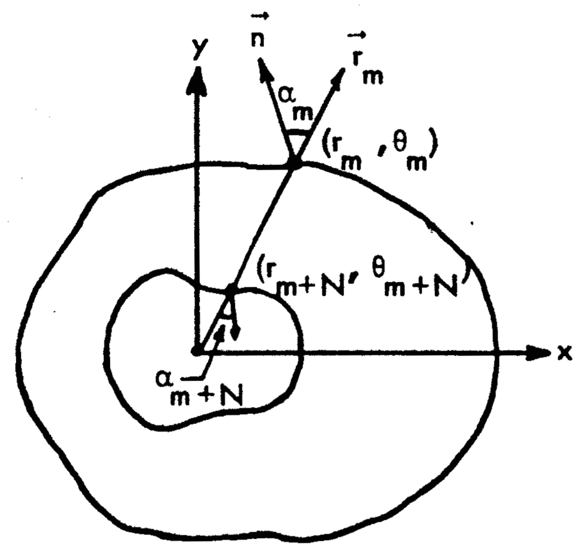

(b)

Fig. 1 (a) The geometry of the two-conductor waveguide under consideration.

(b) The angle α at the chosen points.

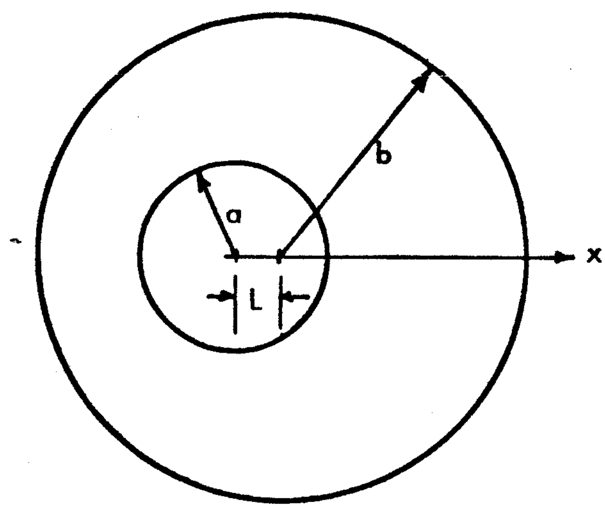

Fig. 2 The cross section of the eccentric waveguide.

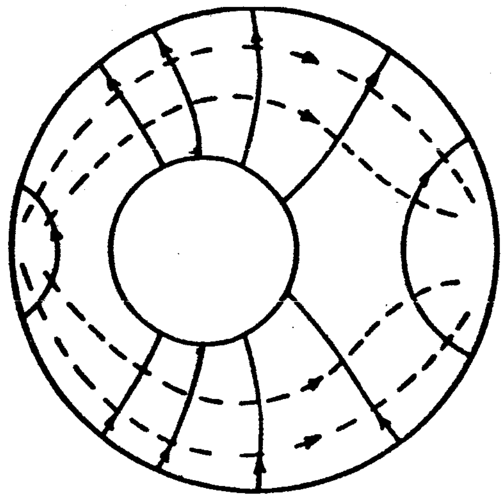

(a)

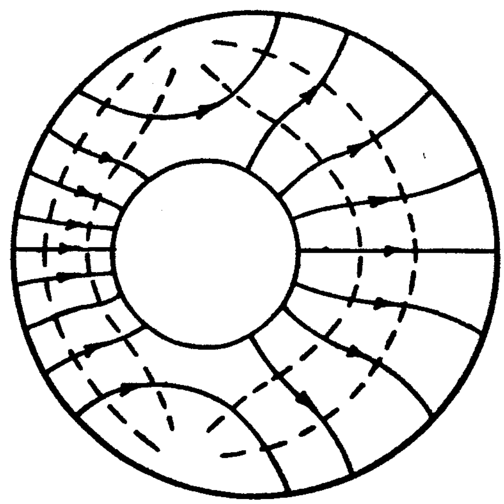

(b)

Fig. 3 (a) The field configuration of the ETE_{11} mode.
(b) The field configuration of the OTE_{11} mode.

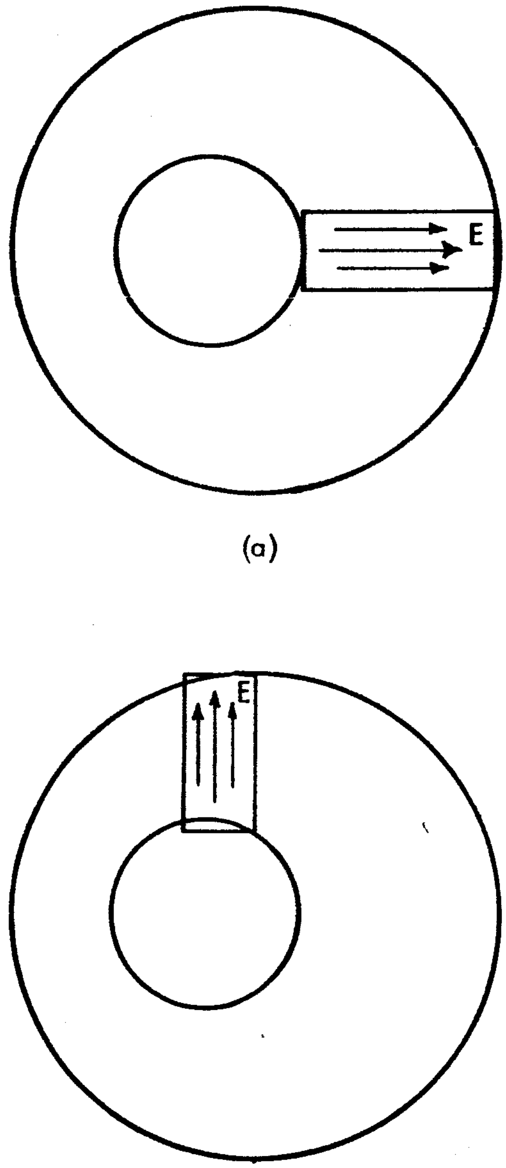

(a)

(b)

Fig. 4 (a) The coupling hole for exciting OTE_{11} mode.
(b) The coupling hole for exciting ETE_{11} mode.
The arrows indicate the electric field of the excitation.

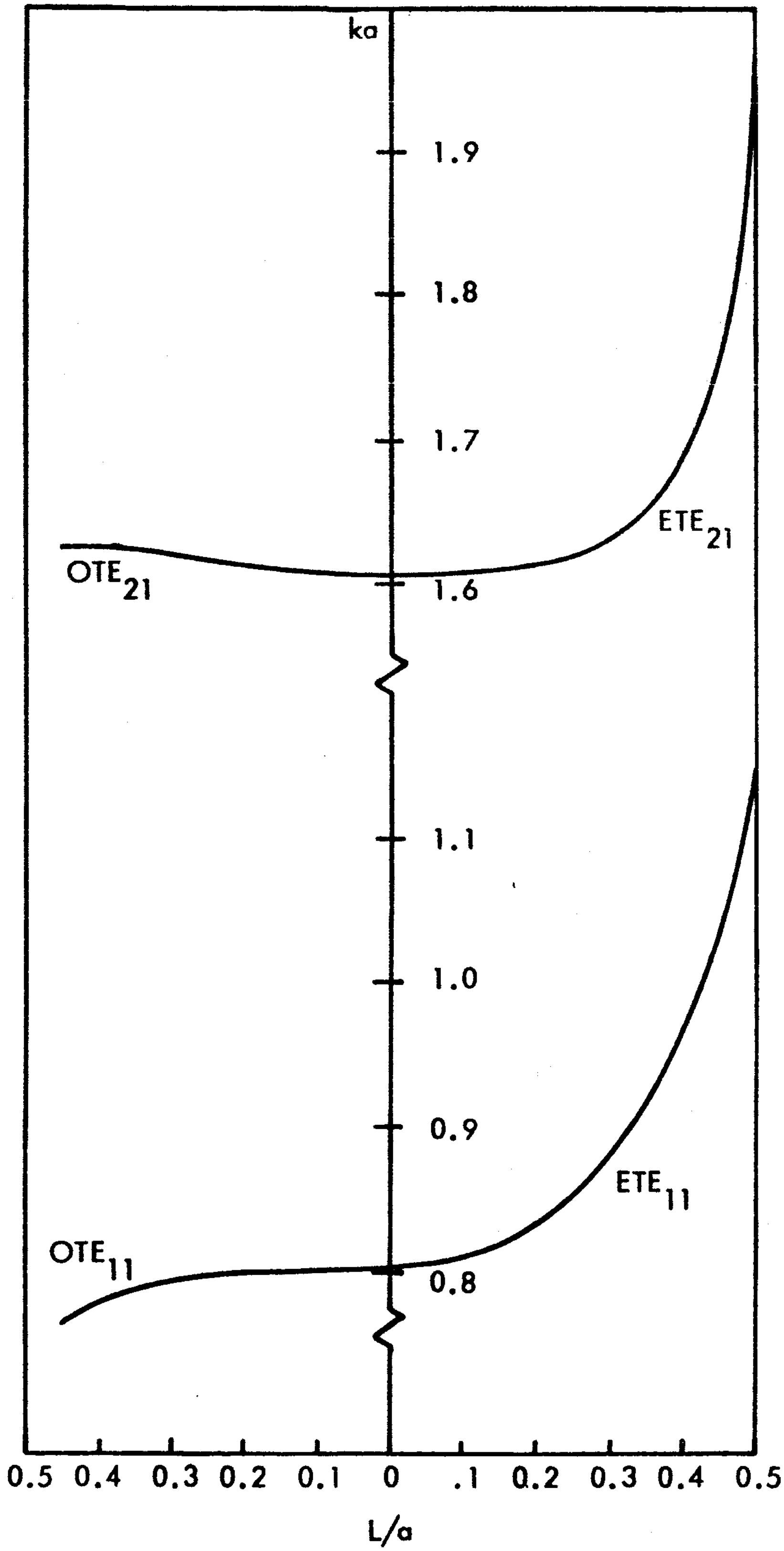

Fig. 5 Cutoff wave numbers of eccentric guide with b/a = 1.5 for TE modes.

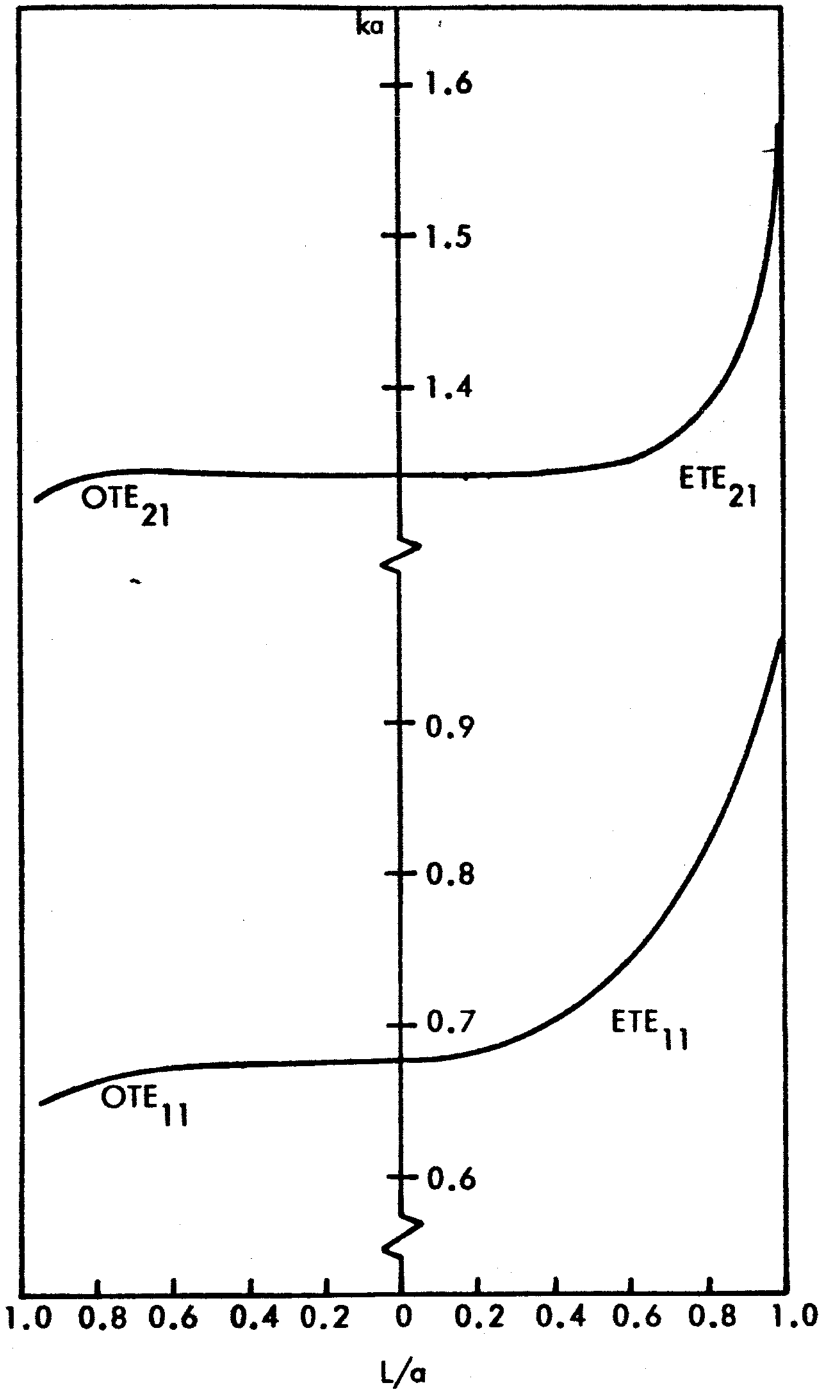

Fig. 6 Cutoff wave numbers of eccentric guide with $b/a = 2.0$ for TE modes.

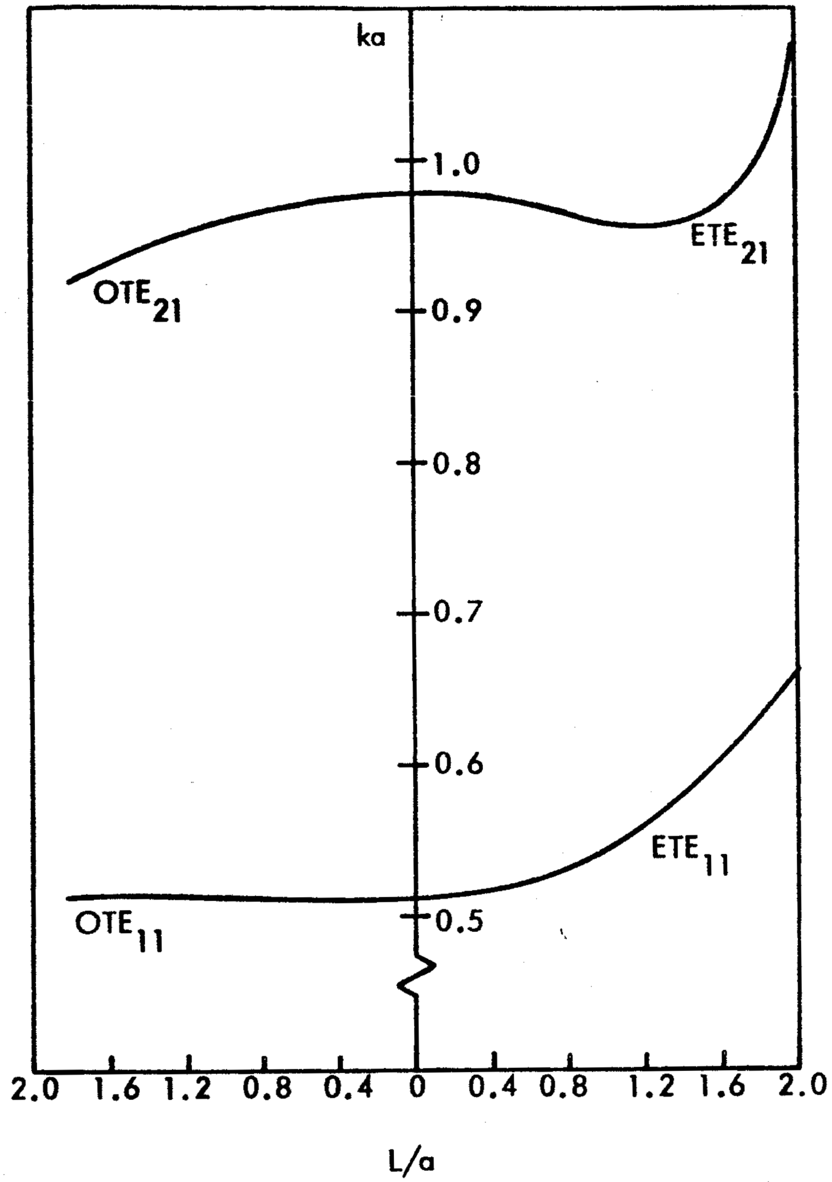

Fig. 7 Cutoff wave numbers of eccentric guide with $b/a = 3.0$ for TE modes.

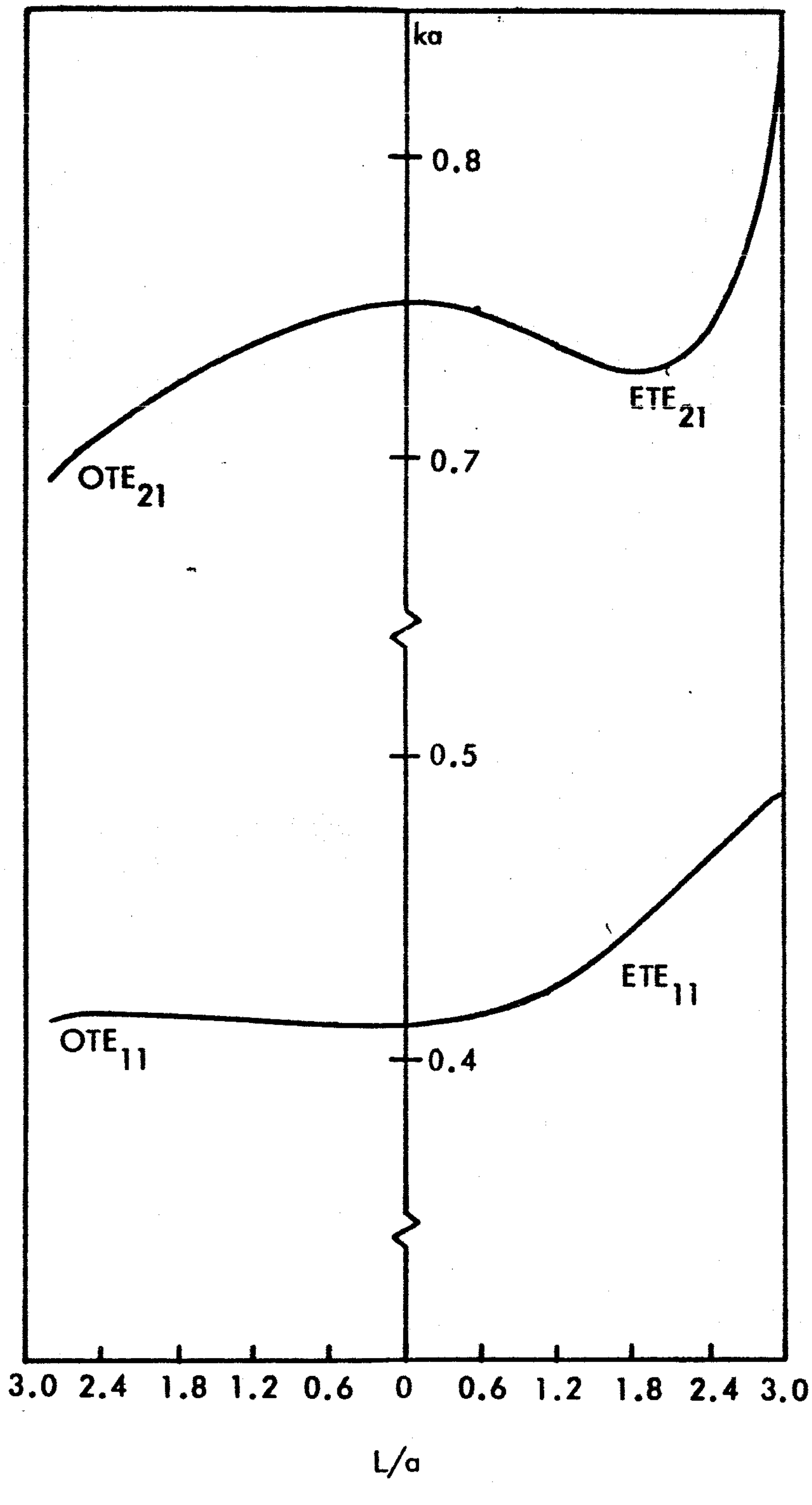

Fig. 8 Cutoff wave numbers of eccentric guide with $b/a = 4$ for TE modes.

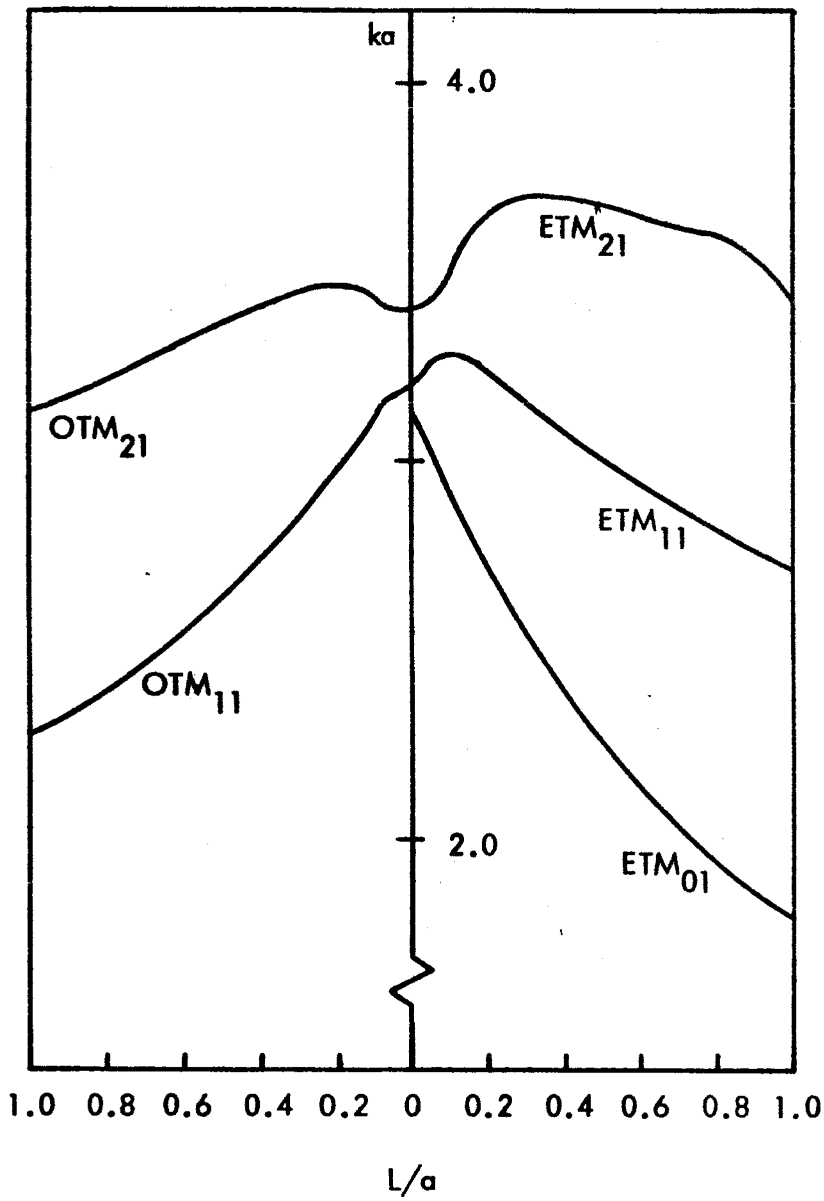

Fig. 9 Cutoff wave numbers of eccentric guide with $b/a = 2.0$ for TM modes.

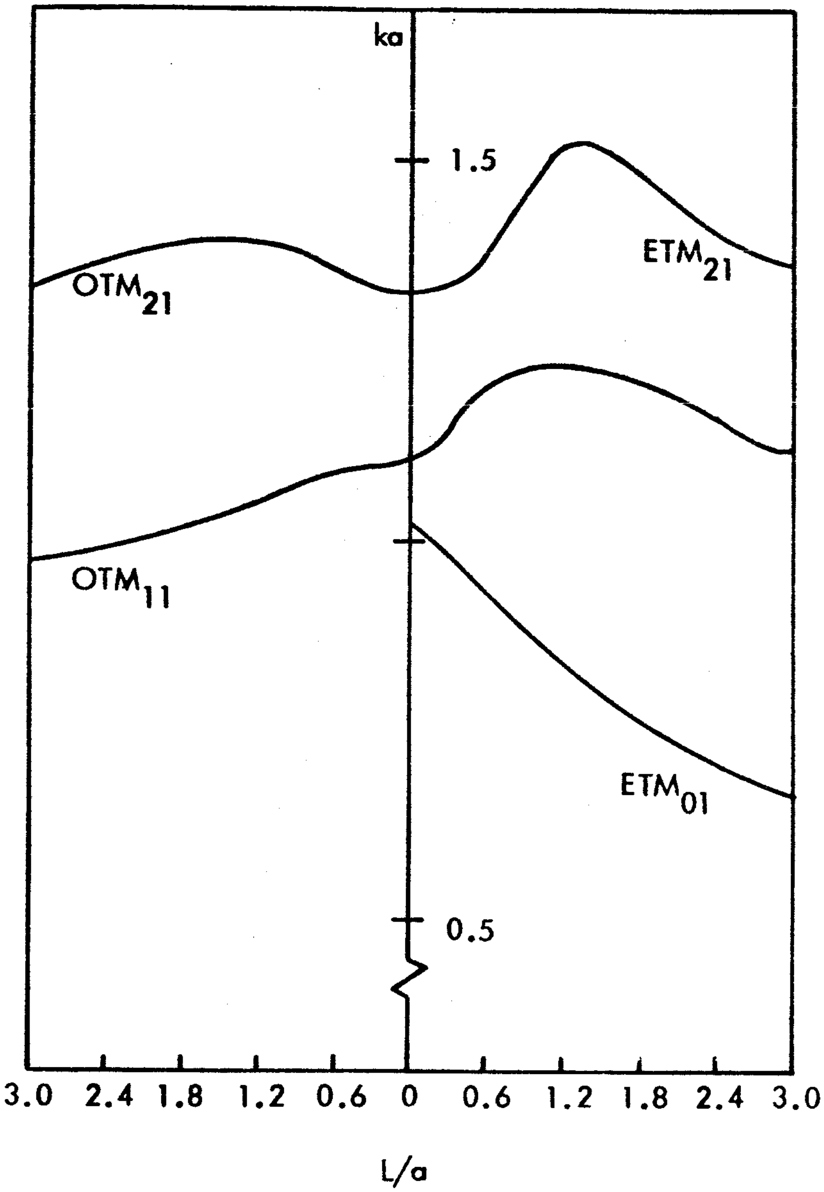

Fig. 10 Cutoff wave numbers of eccentric guide with $b/a = 4$ for TM modes.